



## Original Article

# An examination of the saturation microstructures achieved in ultrafine-grained metals processed by high-pressure torsion<sup>☆</sup>



Shima Sabbaghianrad<sup>a</sup>, Jittraporn Wongsangam<sup>b</sup>, Megumi Kawasaki<sup>a,c,\*</sup>,  
Terence G. Langdon<sup>a,d</sup>

<sup>a</sup> Departments of Aerospace & Mechanical Engineering and Materials Science, University of Southern California, Los Angeles, United States

<sup>b</sup> Department of Mechanical Engineering, Faculty of Engineering, King Mongkut's Institute of Technology Ladkrabang, Bangkok, Thailand

<sup>c</sup> Division of Materials Science and Engineering, Hanyang University, Seoul, South Korea

<sup>d</sup> Materials Research Group, Faculty of Engineering and the Environment, University of Southampton, Southampton, United Kingdom

## ARTICLE INFO

## Article history:

Received 20 May 2014

Accepted 2 October 2014

Available online 8 November 2014

## Keywords:

Aluminum alloy

Copper alloy

Hardness

High-pressure torsion

Ultrafine grains

## ABSTRACT

Experiments were conducted on two commercial alloys, a Cu-0.1%Zr alloy and an Al-7075 aluminum alloy, to investigate the significance of the saturation microstructure which is achieved after processing by high-pressure torsion (HPT). Samples were processed by HPT and also by a combination of equal-channel angular pressing (ECAP) followed by HPT. The results show that the saturation conditions are dependent upon the grain size in the material immediately prior to the HPT processing. Additional grain refinement may be achieved in HPT by initially processing the material to produce an ultrafine-grain size before conducting the processing by HPT.

© 2014 Brazilian Metallurgical, Materials and Mining Association. Published by Elsevier Editora Ltda. Este é um artigo Open Access sob a licença de [CC BY-NC-ND](http://creativecommons.org/licenses/by-nc-nd/4.0/)

## 1. Introduction

It is now well established that it is often advantageous to produce metals having very small grain sizes. This is because if the grain size is small the metal is generally fairly strong

because the yield stress at low temperatures varies with the reciprocal of the square root of the grain size through the Hall-Petch relationship [1,2]. Furthermore, at elevated temperatures small grain sizes provide a potential for achieving a superplastic forming capability [3]. The interest in attaining very small grain sizes led to the development of extensive

<sup>☆</sup> Paper presented in the form of an abstract as part of the proceedings of the Pan American Materials Conference, São Paulo, Brazil, July 21<sup>st</sup> to 25<sup>th</sup> 2014.

\* Corresponding author.

E-mail: [megumi@hanyang.ac.kr](mailto:megumi@hanyang.ac.kr) (M. Kawasaki).

<http://dx.doi.org/10.1016/j.jmrt.2014.10.002>

2238-7854/© 2014 Brazilian Metallurgical, Materials and Mining Association. Published by Elsevier Editora Ltda.

Este é um artigo Open Access sob a licença de [CC BY-NC-ND](http://creativecommons.org/licenses/by-nc-nd/4.0/)

thermo-mechanical processing operations, which were generally effective in producing grain sizes as small as  $\sim 3\text{--}5\ \mu\text{m}$ . Nevertheless, this type of processing was not effective in fabricating metals having grain sizes in the submicrometer range and more recently attention has focused instead on the processing of metals through the application of severe plastic deformation (SPD), where it is possible to achieve grain refinement to the submicrometer and even the nanometer range [4].

Ultrafine-grained materials (UFG) are defined as polycrystals having average grain sizes less than  $1\ \mu\text{m}$  [5]. Thus, UFG structures include both the submicrometer ( $100\ \text{nm}$  to  $1\ \mu\text{m}$ ) and the nanometer ( $<100\ \text{nm}$ ) ranges. These materials may be produced using SPD techniques [6] and accordingly they have attracted much attention over the last two decades. Several different SPD processing methods are now available but the two techniques receiving the most attention are equal-channel angular pressing (ECAP) [7] and high-pressure torsion (HPT) [8]. In ECAP the sample is in the form of a rod or bar and it is pressed through a die constrained within a channel that is bent internally through an abrupt angle. In HPT the sample is generally in the form of a thin disk which is held between massive anvils and then subjected to an applied pressure and concurrent torsional straining. Experiments show that processing by HPT produces both smaller grain sizes and a higher fraction of grain boundaries having high-angles of misorientation than when processing using ECAP [9–11].

The higher strength introduced by SPD processing is demonstrated most effectively by taking individual readings of the Vickers microhardness,  $H_v$ , at selected positions on the polished surfaces of samples processed by either ECAP or HPT. There are now numerous reports describing these measurements recorded on the cross-sectional planes [12–14] and the longitudinal planes [14–16] of ECAP samples and on the surfaces of disks processed by HPT [17–19]. There is a significant problem in using this approach to evaluate homogeneity in HPT because the strain varies across the disk. Specifically, the equivalent von Mises strain,  $\varepsilon_{\text{eq}}$ , is given by a relationship of the form [20,21]

$$\varepsilon_{\text{eq}} = \frac{2\pi Nr}{h\sqrt{3}} \quad (1)$$

where  $N$  is the number of revolutions in HPT processing and  $r$  and  $h$  are the radius and height (or thickness) of the disk, respectively. It follows from Eq. (1) that  $\varepsilon_{\text{eq}}$  is a maximum at the edge of the disk and decreases to zero at the center of the disk where  $r=0$ . There are numerous experiments [10,18] showing a gradual evolution during HPT processing so that the microhardness values become essentially constant over the disk surfaces after a reasonably large number of revolutions. Furthermore, this evolution is also consistent with a theoretical model for hardness evolution in HPT [22].

Nevertheless, questions remain concerning the limits of grain refinement that may be attained through processing by ECAP or HPT [23,24] and at present these questions remain unresolved. Accordingly, this paper examines whether there is a true limitation on the refining of grains when processing by HPT and experiments are described which are designed to

provide a critical examination of the possible occurrence of a true refining limit.

## 2. Experimental materials and procedures

The experiments were conducted by processing in HPT using two different face-centered cubic materials. First, tests were conducted on a commercial Cu-151 alloy with a composition of Cu-0.1wt% Zr. This alloy was obtained from Olin Brass (East Alton, OH) as a rolled strip having dimensions of  $760 \times 500\ \text{mm}^2$  and a thickness of  $1.5\ \text{mm}$ . Disks were machined from the strip with diameters of  $10\ \text{mm}$  and these disks were then polished to thicknesses of  $\sim 0.83\ \text{mm}$ . In the initial unprocessed condition, the measured grain size was  $\sim 20\ \mu\text{m}$ . Earlier reports described the SPD processing of this Cu-Zr alloy [11,14,25–28]. Second, experiments were conducted on a commercial Al-7075 alloy containing (in wt.%) 5.6% Zn, 2.5% Mg, 1.6% Cu with the balance as Al. This alloy was received in the form of extruded rods with diameters of  $10.0\ \text{mm}$  and these rods were annealed in air for 1 h at  $753\ \text{K}$  and then cooled in air to room temperature over a period of  $\sim 5\ \text{min}$ . In the annealed and unprocessed condition, the grains were elongated with lengths up to  $\sim 450\ \mu\text{m}$  and widths of  $\sim 8\ \mu\text{m}$ . This alloy was processed by HPT and also by ECAP and a combination of ECAP and HPT. Earlier reports described the processing of the Al-7075 alloy by SPD techniques [29–31].

For ECAP, the processing was performed at  $473\ \text{K}$  using a solid die with a channel having an internal angle of  $110^\circ$  and an outer arc of curvature of  $20^\circ$ . These angles lead to an imposed strain of  $\sim 0.8$  on each separate passage through the die [32]. The billets were processed using processing route Bc in which the rods are rotated by  $90^\circ$  in the same sense between each pass [33]. Following ECAP through either 4 or 8 passes, disks were cut from some of the billets and then used for processing by HPT: these samples are henceforth designated the ECAP + HPT samples. All HPT processing used disks with diameters of  $10.0\ \text{mm}$  and thicknesses of  $\sim 0.83\ \text{mm}$ . The disks were polished prior to HPT and then processed at room temperature (RT) for selected numbers of revolutions,  $N$ , under an applied pressure of  $6.0\ \text{GPa}$  and with a rotational rate of  $1\ \text{rpm}$ . The HPT processing was conducted under quasi-constrained conditions in which there is a small outflow of material around the periphery of the disk during the processing operation [34,35]. Full details of the HPT processing were given earlier except that a lubricant was not placed on the upper and lower anvils prior to processing [36].

The major emphasis in this investigation was to evaluate the limits of grain refinement under different HPT processing conditions. In practice, however, it is experimentally easier to compare the values of the saturation hardness which are attained by processing since these values relate directly to the microstructures in the materials. Two separate procedures were developed earlier for achieving rigorous measurements of the microhardness values [36] and the same procedures were followed in the present investigation. The principles of these two procedures are illustrated schematically in Fig. 1 [36]. All values of the Vickers microhardness,  $H_v$ , were recorded using a microhardness tester equipped with a Vickers indenter using a load of  $100\ \text{gf}$  and a dwell time of  $15\ \text{s}$

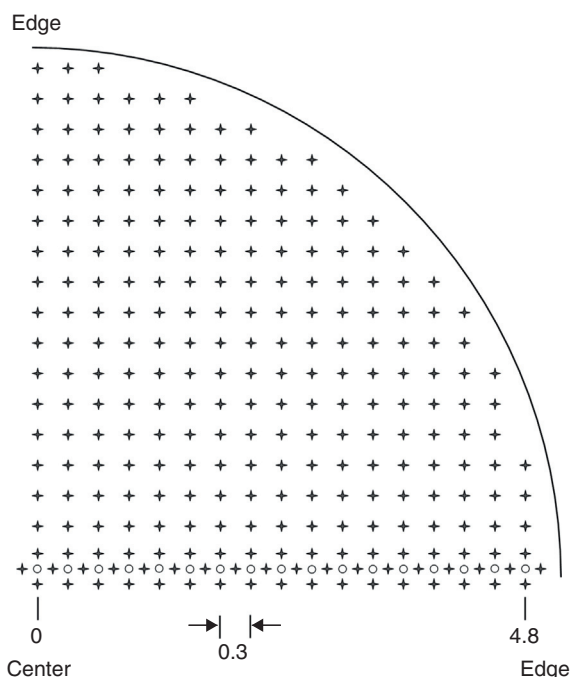


**Fig. 1 – Procedures for recording microhardness values in HPT either along a disk diameter or across one-quarter of the disk surface [36].**

for each measurement. First, the individual hardness values were recorded across the diameters of disks by taking measurements at individual positions separated by distances of 0.3 mm and at each selected position the value of Hv was determined by averaging four measurements from separate points arranged in a cruciform configuration and separated from the selected point by 0.15 mm. Second, measurements of Hv were taken over one-quarter of the disk surface as shown in Fig. 1, with measurements taken at points that follow a rectilinear grid pattern with a separation between points of 0.3 mm. From these measurements, it was possible to construct color-coded contour maps which provide a visual display of the hardness distributions over each surface of the disk after processing.

### 3. Experimental results

#### 3.1. Characteristics of grain refinement in processing by HPT

In order to obtain a meaningful representation of the occurrence of grain refinement in processing by HPT, it follows from Eq. (1) that it is necessary to examine the microstructure both at the center and at the edge of each disk. An example is shown in Fig. 2 for the Cu–Zr alloy processed under an applied pressure of 6.0 GPa: the left column shows images taken in the center of each disk, the right column shows images near the edges, results are displayed after (a) 1/4 turn, (b) 5 turns and (c) 10 turns and the individual colors represent different grain orientations [28]. In Fig. 2(a) the original coarse grains are visible in the center of the disk after 1/4 turn but there is clear grain refinement near the edge. After 5 turns in Fig. 2(b) there is grain

refinement both in the center and at the edge but the average grain size was  $\sim 290$  nm in the center and  $\sim 240$  nm near the edge. Finally, after 10 turns in Fig. 2(c) both the center and the edge are reasonably homogeneous, the grains are essentially equiaxed and the measured average sizes were  $\sim 270$  nm and  $\sim 230$  nm at the center and edge, respectively. Since the initial grain size was  $\sim 20$   $\mu\text{m}$  before processing by HPT, these images confirm the potential for achieving excellent grain refinement through HPT processing.

#### 3.2. Achieving a visual display of the hardness evolution in HPT processing

Microhardness measurements were recorded over one-quarter of each disk of the Al-7075 alloy after processing through 1/2, 1, 2 and 5 turns with a pressure of 6.0 GPa and the results are shown in Fig. 3, where the values of the Vickers microhardness Hv are displayed using a color code indicated at the bottom right [29]. In Fig. 3, the X and Y coordinate system denotes two arbitrarily selected orthogonal axes that lie in the plane of each disk and intersect at the center of the disk at the point given by (0, 0). These diagrams confirm the increasing hardness with increasing numbers of turns and the gradual evolution toward a more equilibrated structure. Thus, after 1/2 turn there is a large area around the central point where the hardness is exceptionally low but this area decreases in size after 1 and 2 turns and essentially disappears after 5 turns. Thus, only 5 turns are needed in order to achieve a reasonable level of homogeneity throughout the disk.

#### 3.3. Measurements of microhardness values taken along linear traverses after processing by HPT

Values of the Vickers microhardness were taken along randomly selected diameters of disks of the Al-7075 alloy processed through various numbers of turns from 1/8 to 10 using the same applied pressure of 6.0 GPa. The results of these measurements are shown in Fig. 4, where the individual points are plotted against the distance from the center of the disk for each testing condition and with the lower dashed line showing the hardness value of  $Hv \approx 102$  in the alloy after annealing but prior to HPT processing [29]. These results show that the hardness gradually increases with increasing numbers of turns, this increase occurs initially most rapidly at the edges of the disks but ultimately, after 10 turns, similar values of Hv are attained across the disk diameter. After 10 turns, the hardness appears to be reasonably saturated at all points across the disk.

The experimental points in Fig. 4 tend to be scattered but it was noted in a very early investigation of HPT that it should be possible to correlate these various points by plotting the data in the form of the values of Hv against the equivalent strain as calculated from Eq. (1) and this type of plot should also provide a direct measure of the saturation hardness [37]. When the datum points in Fig. 4 are replotted in this way, the result is shown in Fig. 5 where the 95% error bars are included at the highest equivalent strains [30]. Thus, the hardness increases up to an equivalent strain of  $\sim 50$ , and thereafter there is only a minor increase in hardness and ultimately the hardness saturates at  $Hv \approx 230$ .

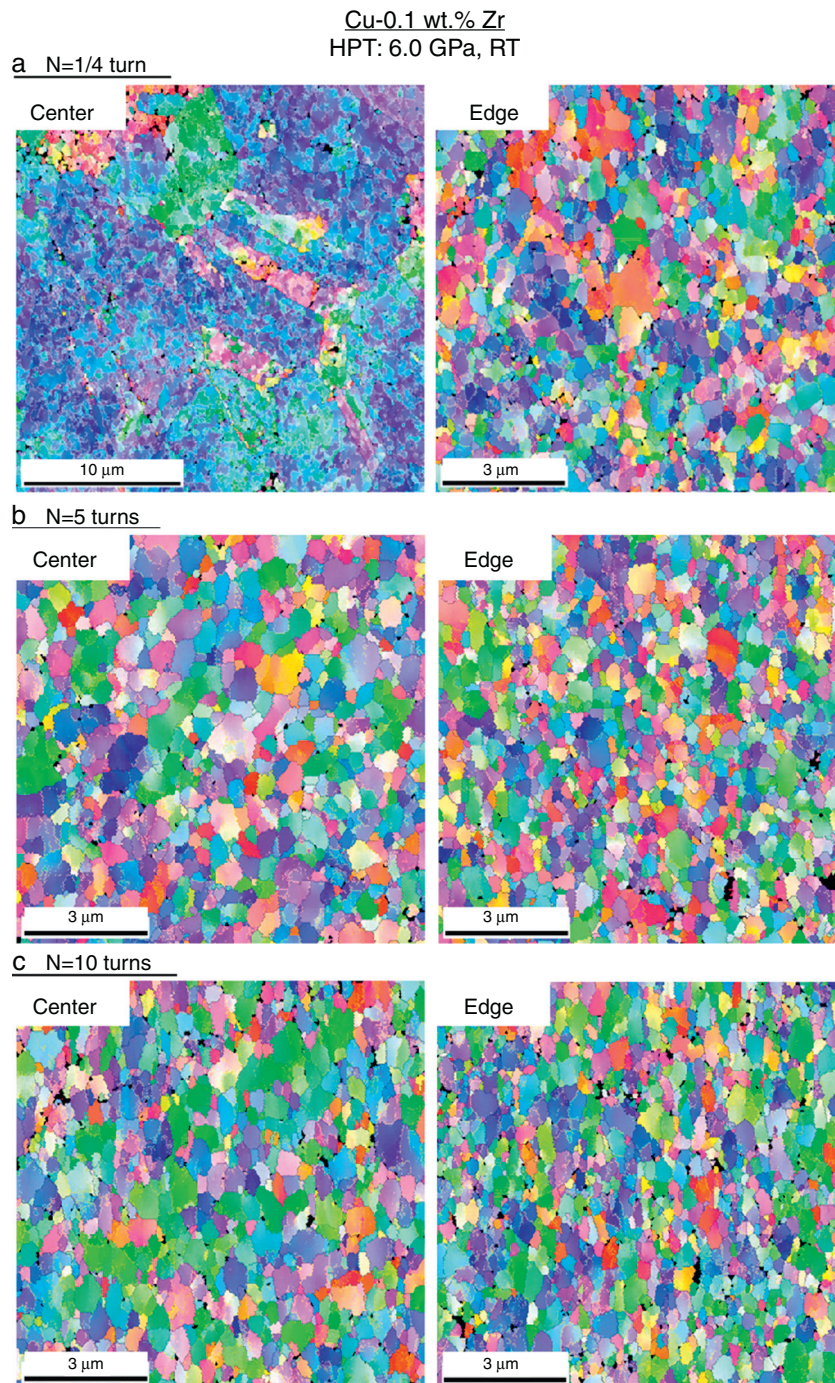


**Fig. 2 – Grain refinement in the Cu-Zr alloy after processing by HPT with a pressure of 6.0 GPa: images are shown for the center and edge of the disk after (a) 1/4 turn, (b) 5 turns and (c) 10 turns [28].**

### 3.4. The influence on hardness of an initial processing by ECAP

The preceding results in Section 3.3 show that the as-annealed Al-7075 alloy attains a saturation hardness of  $H_v \approx 230$  when processing in the conventional manner. However, additional experiments were needed to determine whether this saturation value is affected by the initial microstructural condition immediately before the HPT processing. Accordingly, samples

were processed by ECAP through either 4 or 8 passes at a temperature of 473 K prior to conducting the HPT processing.

The results are shown in Fig. 6 [30] and Fig. 7 for samples processed through either 4 or 8 passes of ECAP, respectively, and then processed by HPT with an applied pressure of 6.0 GPa. In Fig. 6 for 4 passes of ECAP, the points again increase very rapidly in the initial stages but ultimately there is a saturation at  $H_v \approx 250$ . By contrast, in Fig. 7 after 8 passes of ECAP the saturation hardness occurs at a higher value of  $H_v \approx 270$ .

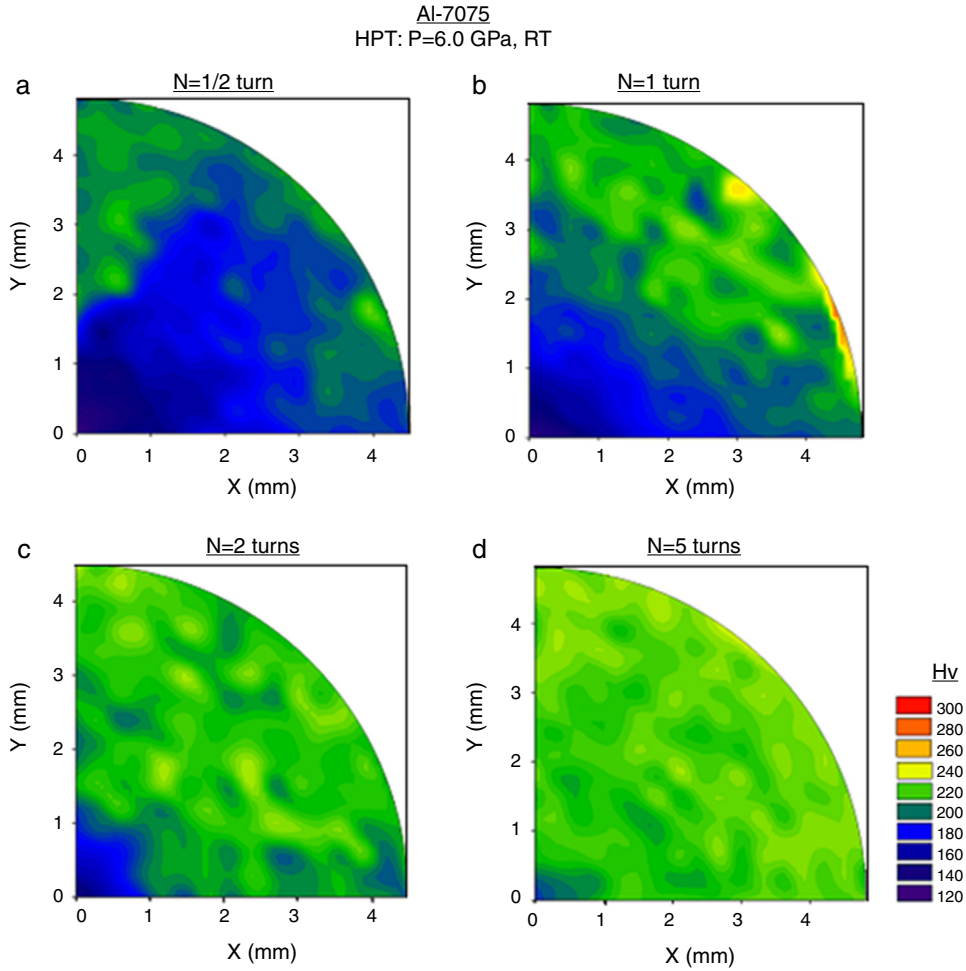


Fig. 3 – Color-coded displays showing the evolution in hardness in the Al-7075 alloy over one-quarter of the disk surfaces after processing by HPT with a pressure of 6.0 GPa for (a) 1/2 turn, (b) 1 turn, (c) 2 turns and (d) 5 turns [29].

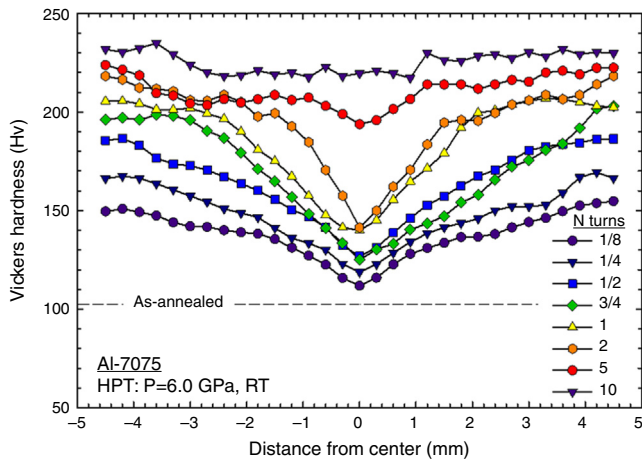


Fig. 4 – Variation of the Vickers microhardness across disk diameters of the Al-7075 alloy after processing by HPT through different numbers of turns using a pressure of 6.0 GPa [29].

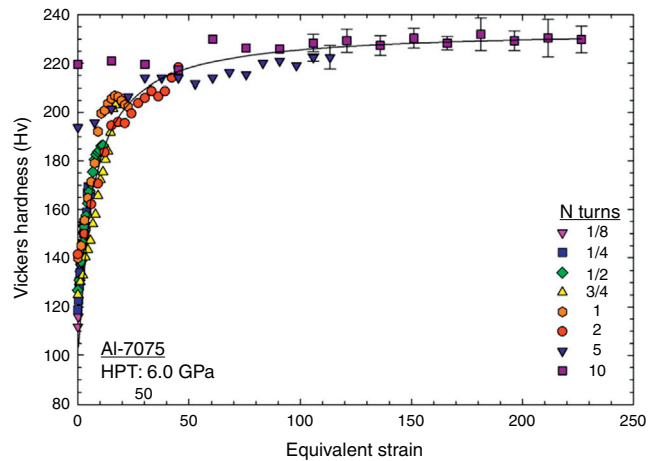
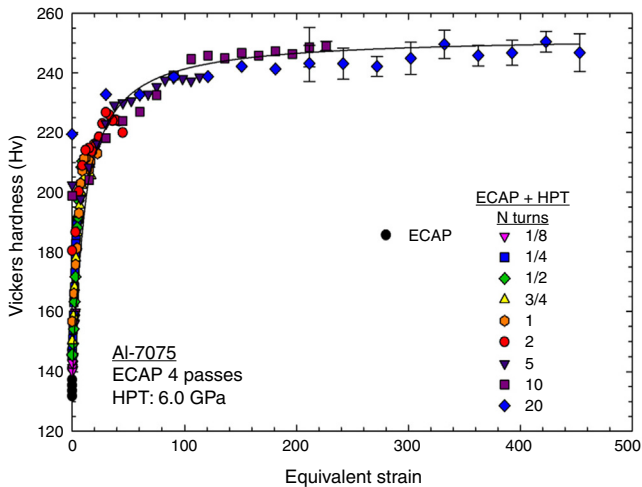


Fig. 5 – Values of the Vickers microhardness plotted against the equivalent strain after processing the Al-7075 alloy by HPT using a pressure of 6.0 GPa [30].



**Fig. 6** – Values of the Vickers microhardness plotted against the equivalent strain after processing the Al-7075 alloy by ECAP for 4 passes and then by HPT using a pressure of 6.0 GPa [30].

#### 4. Discussion

It is generally assumed that the factors influencing the saturation hardness attained in HPT are dependent upon the experimental processing conditions. Specifically, it is assumed that the hardness, and therefore the saturation grain size, depends upon the applied pressure in HPT, the temperature of processing and possibly upon the rate of rotation of the HPT anvil although experiments suggest this rate probably has only a relatively minor influence [38]. An expression was developed for the minimum grain size that may be produced in HPT and inspection shows that this relationship incorporates some features that relate to the initial unprocessed condition such as the dislocation density and the yield stress [39]. A similar approach was also developed later for processing by ECAP [40]. Nevertheless, there is no clear and definitive relationship

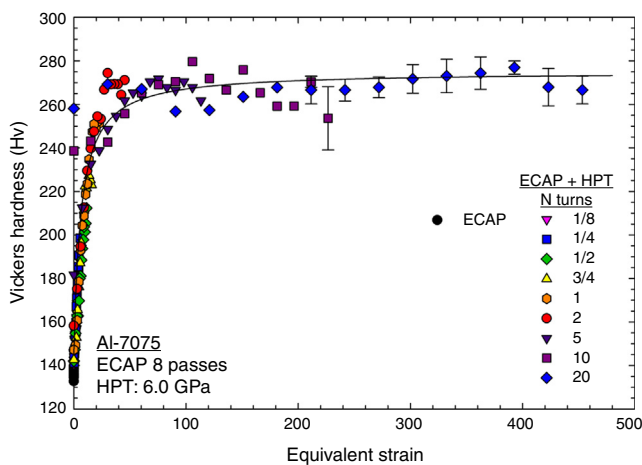


**Fig. 7** – Values of the Vickers microhardness plotted against the equivalent strain after processing the Al-7075 alloy by ECAP for 8 passes and then by HPT using a pressure of 6.0 GPa.

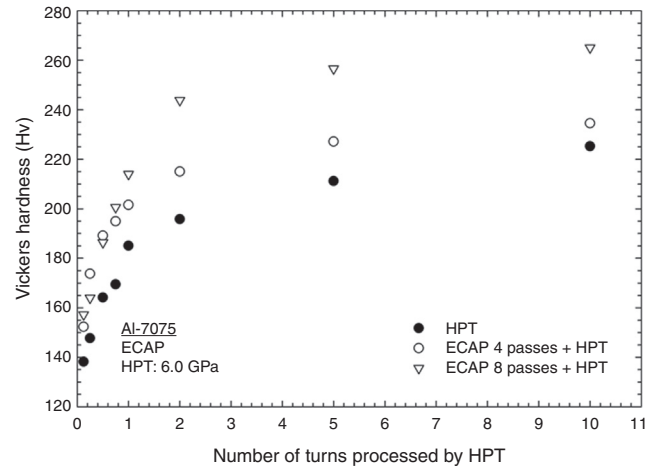


**Fig. 8** – Plots of the average Vickers microhardness across diameters of the disks of the Al-7075 alloy after processing by HPT and by ECAP + HPT.

that specifically dictates the saturation conditions that may be attained after a combination of processing by ECAP and HPT.

In the present investigation, there is a clear difference between the saturation hardnesses achieved in the Al-7075 alloy after three different testing conditions. For HPT with  $P=6.0$  GPa the hardness saturates at  $Hv \approx 230$ , for ECAP through 4 passes and then the same conditions for HPT, there is a saturation at  $Hv \approx 250$  and for ECAP through 8 passes and then the same HPT, there is a saturation at  $Hv \approx 270$ . The 95% error bars in Figs. 5–7 are sufficiently small to unequivocally establish these differences in the values of Hv. Furthermore, it is possible to plot the results in a different way by noting that the numbers of hardness measurements are the same across the diameters of each disk and therefore it is possible to simply average these measurements for each processing condition and then to plot the average value of the Vickers microhardness against the total numbers of turns in HPT. The result is shown in Fig. 8 for the disks processed only by HPT and for the disks processed initially by ECAP through either 4 or 8 passes prior to HPT. It is readily apparent that all points for the HPT samples have the lowest values and the points for the ECAP + HPT disks show higher values of Hv. This confirms that, as is evident from Figs. 5–7, additional hardening, and therefore additional grain refinement, may be achieved by processing the material prior to HPT in order to achieve an even smaller initial grain size.

It is important to note that the initial microstructural condition prior to the two-step processing by ECAP + HPT is critical in order to demonstrate both additional hardening and grain refinement. For example, a recent report demonstrated there were lower saturated hardness values in an Al-6082 disk after ECAP + HPT by comparison with a disk processed only by HPT when using the same HPT processing conditions. This difference was due to the presence of an over-aged microstructure in the initial samples prior to ECAP and HPT because the samples were solution treated for 2 h at 843 K and then aged at 573 K for 3 h before processing by ECAP [41]. This contrasts with the present experiments where the samples were not aged prior to processing by ECAP or HPT.

When materials are processed by HPT, most metals, including many face-centered cubic metals, exhibit a simple strain hardening behavior without any significant recovery [42]. The Cu–Zr alloy and the Al-7075 alloy are typical of this group of materials as shown in Figs. 5–7. However, some other materials exhibit different behavior including strain hardening with recovery in high-purity aluminum [17] and strain softening with respect to the initial condition in some two-phase alloys [43,44]. A full description of these various hardening models is given elsewhere [42]. However, additional experiments are now needed to determine whether these other materials also exhibit saturation hardness values, and minimum grain sizes, that vary depending upon the precise nature of the processing conditions as, for example, in processing using a combination of ECAP and HPT.

## 5. Summary and conclusions

1. A Cu–Zr alloy and an aluminum Al-7075 alloy were used to investigate grain refinement and the evolution of hardness homogeneity during processing by HPT.
2. Results on the Al-7075 alloy show that the saturation hardness is dependent upon the microstructural conditions within the material prior to processing. Higher values of saturation hardness are attained if the same material is processed by ECAP prior to HPT.
3. Since the measured values of the microhardness are related directly to the grain size, the results demonstrate that additional grain refinement may be achieved in HPT by processing the material to produce an ultrafine-grain size before processing by HPT.

## Conflict of interest

The authors declare no conflicts of interest.

## Acknowledgements

This work was supported in part by the research fund of Hanyang University (HY-2013), in part by the National Science Foundation of the United States under Grant No. DMR-1160966 and in part by the European Research Council under ERC Grant Agreement No. 267464-SPDMETALS.

## REFERENCES

- [1] Hall EO. The deformation and ageing of mild steel: III. discussion of results. *Proc Phys Soc B* 1951;64:747–53.
- [2] Petch NJ. Cleavage strength of polycrystals. *J Iron Steel Inst* 1953;174:25–8.
- [3] Langdon TG. Seventy-five years of superplasticity: historic developments and new opportunities. *J Mater Sci* 2009;44:5998–6010.
- [4] Valiev RZ, Islamgaliev RK, Alexandrov IV. Bulk nanostructured materials from severe plastic deformation. *Prog Mater Sci* 2000;45:103–89.
- [5] Valiev RZ, Estrin Y, Horita Z, Langdon TG, Zehetbauer MJ, Zhu YT. Producing bulk ultrafine-grained materials by severe plastic deformation. *JOM* 2006;58(4):33–9.
- [6] Langdon TG. Twenty-five years of ultrafine-grained materials: achieving exceptional properties through grain refinement. *Acta Mater* 2013;61:7035–59.
- [7] Valiev RZ, Langdon TG. Principles of equal-channel angular pressing as a processing tool for grain refinement. *Prog Mater Sci* 2006;51:881–981.
- [8] Zhilyaev AP, Langdon TG. Using high-pressure torsion for metal processing: fundamentals and applications. *Prog Mater Sci* 2008;53:893–979.
- [9] Zhilyaev AP, Kim BK, Nurislamova GV, Baró MD, Szpunar JA, Langdon TG. Orientation imaging microscopy of ultrafine-grained nickel. *Scripta Mater* 2002;46:575–80.
- [10] Zhilyaev AP, Nurislamova GV, Kim BK, Baró MD, Szpunar JA, Langdon TG. Experimental parameters influencing grain refinement and microstructural evolution during high-pressure torsion. *Acta Mater* 2003;51: 753–65.
- [11] Wongsangam J, Kawasaki M, Langdon TG. A comparison of microstructures and mechanical properties in a Cu–Zr alloy processed using different SPD techniques. *J Mater Sci* 2013;48:4653–60.
- [12] Xu C, Furukawa M, Horita Z, Langdon TG. The evolution of homogeneity and grain refinement during equal-channel angular pressing: a model for grain refinement in ECAP. *Mater Sci Eng* 2005;A398:66–76.
- [13] Xu C, Xia K, Langdon TG. The role of back pressure in the processing of pure aluminum by equal-channel angular pressing. *Acta Mater* 2007;55:2351–60.
- [14] Wongsangam J, Kawasaki M, Langdon TG. The development of hardness homogeneity in a Cu–Zr alloy processed by equal-channel angular pressing. *Mater Sci Eng* 2012;A556:526–32.
- [15] Prell M, Xu C, Langdon TG. The evolution of homogeneity on longitudinal sections during processing by ECAP. *Mater Sci Eng* 2008;A480:449–55.
- [16] Vevečka A, Cabibbo M, Langdon TG. A characterization of microstructure and microhardness on longitudinal planes of an Al–Mg–Si alloy processed by ECAP. *Mater Charact* 2013;84:126–33.
- [17] Xu C, Horita Z, Langdon TG. The evolution of homogeneity in processing by high-pressure torsion. *Acta Mater* 2007;55:203–12.
- [18] Kawasaki M, Figueiredo RB, Langdon TG. An investigation of hardness homogeneity throughout disks processed by high-pressure torsion. *Acta Mater* 2011;59:308–16.
- [19] Kawasaki M, Alhajeri SN, Xu C, Langdon TG. The development of hardness homogeneity in pure aluminum and aluminum alloy disks processed by high-pressure torsion. *Mater Sci Eng* 2011;A529:345–51.
- [20] Valiev RZ, Ivanisenko YuV, Rauch EF, Baudelet B. Structure and deformation behaviour of Armco iron subjected to severe plastic deformation. *Acta Mater* 1996;44:4705–12.
- [21] Wetscher F, Vorhauer A, Stock R, Pippan R. Structural refinement of low alloyed steels during severe plastic deformation. *Mater Sci Eng* 2004;A387–389:809–16.
- [22] Estrin Y, Molotnikov A, Davies CHJ, Lapovok R. Strain gradient modeling of high-pressure torsion. *J Mech Phys Solids* 2008;56:1186–202.
- [23] Pippan R, Wetscher F, Hafok M, Vorhauer A, Sabirov I. The limits of refinement by severe plastic deformation. *Adv Eng Mater* 2006;8:1046–56.
- [24] Pippan R, Scheriau S, Taylor A, Hafok M, Hohenwarter A, Bachmaier A. Saturation of fragmentation during severe plastic deformation. *Ann Rev Mater Res* 2010;40:319–43.
- [25] Wongsangam J, Kawasaki M, Langdon TG. Microstructural evolution and mechanical properties of a Cu–Zr alloy

- processed by high-pressure torsion. *Mater Sci Eng* 2011;A528:7715–22.
- [26] Wongsan-Ngam J, Kawasaki M, Langdon TG. Achieving homogeneity in a Cu–Zr alloy processed by high-pressure torsion. *J Mater Sci* 2012;47:7782–8.
- [27] Wongsan-Ngam J, Wen H, Langdon TG. Microstructural evolution in a Cu–Zr alloy processed by a combination of ECAP and HPT. *Mater Sci Eng* 2013;A579:126–35.
- [28] Wongsan-Ngam J, Langdon TG. Microstructural evolution and grain refinement in a Cu–Zr alloy processed by high-pressure torsion. *Mater Sci Forum* 2014;783–786:2635–40.
- [29] Sabbaghianrad S, Kawasaki M, Langdon TG. Microstructural evolution and the mechanical properties of an aluminum alloy processed by high-pressure torsion. *J Mater Sci* 2012;47:7789–95.
- [30] Sabbaghianrad S, Langdon TG. A critical evaluation of the processing of an aluminum 7075 alloy using a combination of ECAP and HPT. *Mater Sci Eng* 2014;A596:52–8.
- [31] Sabbaghianrad S, Langdon TG. An investigation of mechanical properties and microstructural evolution in an aluminum alloy processed by severe plastic deformation. *Adv Mater Res* 2014;922:610–5.
- [32] Iwahashi Y, Wang J, Horita Z, Nemoto M, Langdon TG. Principle of equal-channel angular pressing for the processing of ultrafine-grained materials. *Scripta Mater* 1996;35:143–6.
- [33] Furukawa M, Iwahashi Y, Horita Z, Nemoto M, Langdon TG. The shearing characteristics associated with equal-channel angular pressing. *Mater Sci Eng* 1998;A257:328–32.
- [34] Figueiredo RB, Cetlin PR, Langdon TG. Using finite element modeling to examine the flow processes in quasi-constrained high-pressure torsion. *Mater Sci Eng* 2011;A528:8198–204.
- [35] Figueiredo RB, Pereira PHR, Aguilar MTP, Cetlin PR, Langdon TG. Using finite element modeling to examine the temperature distribution in quasi-constrained high-pressure torsion. *Acta Mater* 2012;60:3190–8.
- [36] Kawasaki M, Langdon TG. The significance of strain reversals during processing by high-pressure torsion. *Mater Sci Eng* 2008;A498:341–8.
- [37] Vorhauer A, Pippan R. On the homogeneity of deformation by high pressure torsion. *Scripta Mater* 2004;51:921–5.
- [38] Serre P, Figueiredo RB, Gao N, Langdon TG. Influence of strain rate on the characteristics of a magnesium alloy processed by high-pressure torsion. *Mater Sci Eng* 2011;A528:3601–8.
- [39] Mohamed FA, Dheda SS. On the minimum grain size attainable by high-pressure torsion. *Mater Sci Eng* 2012;A558:59–63.
- [40] Mohamed FA, Dheda SS. On the minimum grain size attainable by equal channel angular pressing. *Mater Sci Eng* 2013;A580:227–30.
- [41] El-Danaf E, Kawasaki M, El-Rayes M, Baig M, Mohammed JA, Langdon TG. Mechanical properties and microstructure evolution in an aluminum 6082 alloy processed by high-pressure torsion. *J Mater Sci* 2014;49:6597–607.
- [42] Kawasaki M. Different models of hardness evolution in ultrafine-grained materials processed by high-pressure torsion. *J Mater Sci* 2014;49:18–34.
- [43] Kawasaki M, Ahn B, Langdon TG. Microstructural evolution in a two-phase alloy processed by high-pressure torsion. *Acta Mater* 2010;58:919–30.
- [44] Zhang NX, Kawasaki M, Huang Y, Langdon TG. Microstructural evolution in two-phase alloys processed by high-pressure torsion. *J Mater Sci* 2013;48:4582–91.